Biomaterials 34 (2013) 5107–5116

Contents lists available at SciVerse ScienceDirect

Biomaterials

journal homepage: www.elsevier.com/locate/biomaterials

# Promotion of neuronal differentiation of neural progenitor cells by using EGFR antibody functionalized collagen scaffolds for spinal cord injury repair

Xiaoran Li [a,1], Zhifeng Xiao [b,1], Jin Han [b], Lei Chen [b], Hanshan Xiao [b], Fukai Ma [c], Xianglin Hou [b], Xing Li [b], Jie Sun [a], Wenyong Ding [d], Yannan Zhao [b], Bing Chen [b], Jianwu Dai [a,b,*]

[a] Division of Nanobiomedicine, Suzhou Institute of Nano-Tech and Nano-Bionics, Chinese Academy of Sciences, Suzhou 215123, China
[b] Key Laboratory of Molecular Developmental Biology, Institute of Genetics and Developmental Biology, Chinese Academy of Sciences, Beijing 100080, China
[c] Department of Neurosurgery, Southern Medical University, Guangzhou 510515, China
[d] Department of Biochemistry, Dalian Medical University, Dalian 116044, China

ARTICLE INFO

*Article history:*
Received 26 February 2013
Accepted 25 March 2013
Available online 13 April 2013

*Keywords:*
Collagen scaffold
EGFR antibody functionalization
Neural progenitor cells
Neuronal differentiation
Myelin proteins
Spinal cord injury repair

ABSTRACT

The main challenge for neural progenitor cell (NPC)-mediated repair of spinal cord injury (SCI) is lack of favorable environment to direct its differentiation towards neurons rather than glial cells. The myelin associated inhibitors have been demonstrated to promote NPC differentiation into glial lineage. Herein, to inhibit the downstream signaling activated by myelin associated inhibitors, cetuximab, an epidermal growth factor receptor (EGFR) neutralizing antibody, functionalized collagen scaffold has been developed as a vehicle for NPC implantation. It was found that collagen-cetuximab 1 μg scaffolds enhanced neuronal differentiation and inhibited astrocytic differentiation of NPCs exposed to myelin proteins significantly *in vitro*. To test the therapeutic effect *in vivo*, NPCs expressing green fluorescent protein (GFP)-embedded scaffolds have been implanted into the 4 mm-long hemisection lesion of rats. We found that the collagen-cetuximab 5 μg scaffolds induced neuronal differentiation and decreased astrocytic differentiation of NPCs, enhanced axon regeneration, and promoted functional recovery markedly. A well-functionalized scaffold was constructed to improve the recovery of SCI, which could promote the neuronal differentiation of neural progenitor cells *in vivo*.



## 1. Introduction

Spinal cord injury (SCI) repair has remained one of the most challenging clinical problems. To date, clinical therapies are largely ineffective. Over recent years, neural progenitor cells (NPCs) are considered to be promising in cell replacement strategies given their propensity to differentiate into neurons and glia, and to repopulate lost or damaged cells and tissues [1]. However, any attempt at functional recovery is met with failure as the grafted NPCs tend to differentiate predominantly into glia rather than neurons [2]. It has been demonstrated that the predisposition for glial differentiation of NPCs was largely due to the inhibitory environment in the lesion site following SCI where physicochemical signals are vital for proper cell fate [3]. Thus, for successful SCI repair, reconstruction of three-dimensional (3D) extracellular environment for grafted cells is becoming increasingly attractive.

The advance in tissue engineering provides an exciting regenerative strategy to engineer stem cell niche. Functionalization of scaffolds with bioactive factors, ECM adhesion proteins, peptides or antagonists could improve stem cell therapies by providing a defined microenvironment during transplantation [4]. Stabenfeldt et al. developed a methylcellulose scaffold functionalized with laminin-1, which supported neuronal and oligodendrocyte differentiation with minimal astrocyte differentiation of neural stem cells [5]. More recently, Lu et al. demonstrated that neural stem cell embedded in fibrin matrices containing growth factor cocktails could differentiate into multiple cellular phenotypes, including 28% of neurons [6]. Despite some promising results, the work of

* Corresponding author. Suzhou Institute of Nano-Tech and Nano-Bionics, Chinese Academy of Sciences, 398 Ruoshui Road, Suzhou Industrial Park, Suzhou 215123, China. Tel.: +86 512 62872766; fax: +86 512 62872546.
*E-mail address:* jwdai@genetics.ac.cn (J. Dai).
[1] These authors contributed equally to this work.

0142-9612/$ – see front matter © 2013 Elsevier Ltd. All rights reserved.
http://dx.doi.org/10.1016/j.biomaterials.2013.03.062

functionalized tissue-engineering scaffolds suitable for NPC implantation is still in an early stage.

Accumulating evidence suggests that myelin-associated proteins such as Nogo, myelin associated glycoprotein (MAG), and oligodendrocyte-myelin glycoprotein (OMgp), have shown inhibitory properties in SCI regeneration [7]. Our previous work has demonstrated that myelin proteins could induce astroglial differentiation of NPCs rather than neuronal differentiation [8]. Numerous studies have demonstrated that down-regulation of Nogo recptor (NgR), the common receptor of myelin-associated inhibitors, could promote axon regeneration [9] and induce differentiation of grafted NPCs into neurons and oligodendrocytes [10]. In recent years, the study on blockade of epidermal growth factor receptor (EGFR) in central nervous system (CNS) injury repair has been motivated by a pioneering work that the inhibition of EGFR blocked the activities of myelin inhibitors on neurite growth and enabled limited regeneration of optic nerve axons. They also demonstrated the underlying signaling mechanism that transactivation of EGFR is the downstream of NgR activated by myelin associated inhibitors and myelin inhibitors triggered the phosphorylation of EGFR in a calcium-dependent manner [11]. Our previous study showed that addition of EGFR antibody 151IgG on the collagen scaffold provided effective stimulation effect on axon growth and neural regeneration in an extreme rat spinal cord injury model [12]. Additionally, it was found that inhibition of EGFR signaling reduced microglial inflammatory response [13] and attenuated reactive astrogliosis [14], resulting in functional outcome after SCI. Also, a recent study revealed that activated EGFR blocked neuronal differentiation and promoted glial fate in NPCs [15]. These evidences demonstrated that EGFR inhibition may be beneficial to CNS trauma [16]. To date, despite the successful trial of EGFR antagonists to promote axon growth and suppress astrocyte activation, their use for NPC fate regulation has not been reported.

In this work, a new type of scaffold comprised of cetuximab, an EGFR antagonist, functionalized porous collagen scaffold is presented. The potential of functionalized collagen scaffold to regulate NPC differentiation was investigated *in vitro* in presence of myelin proteins, and subsequently the therapeutic effect of scaffolds embedded with NPCs expressing green fluorescent protein (GFP) was evaluated in the rat hemisection SCI model.

## 2. Materials and methods

### 2.1. Fabrication of collagen and collagen-cetuximab scaffolds

Collagen (Col) scaffolds were produced by freeze-dried dispersions under acidic conditions as the following procedure. Collagen (Zhenghai Biotechnology Ltd., Shandong, China) was dissolved in 0.5 M acetic acid for 8 h at 4 °C, and homogenized in a blender for 15 min, followed by neutralization with 4 M NaOH. The homogenous solution was dialyzed against deionized water for 5 days to remove any residual salts and then lyophilized.

For preparation of collagen-cetuximab (col-cetuximab) scaffolds, chemical conjugation of cetuximab to collage scaffold was performed by two-step reactions with sulfo-succinimidyl derivatives (Sulfo-SMCC) (Sigma, USA) and Traut's Reagent (Sigma, USA), as the following. Collagen scaffold was immersed in 2.5 mg/mL of Traut's Reagent in PBS with 4 mM EDTA (pH = 8) for 2 h at room temperature (RT). In a separate reaction, 2.5 mg of Sulfo-SMCC was dissolved in 4 mL of PBS with 4 mM EDTA (pH = 7.2), and then cetuximab was added into the Sulfo-SMCC solution with a ratio of 8:3.7 (μg/μL) followed by reaction for 1 h at RT. The collagen scaffolds treated by Traut's Reagent was washed with PBS for three times and incubated with the cetuximab solution for 1 h at RT. Subsequently, the collagen scaffolds were washed by PBS for three times, and incubated with 5% (W/V) bovine serum albumin (BSA) (Sigma, USA) for 1 h to block remaining reaction groups.

### 2.2. Quantification of cetuximab by enzyme-linked immunosorbent (ELISA) assay

Cetuximab adsorbed or conjugated on scaffolds was quantified by ELISA assay. Goat anti-mouse-alkaline phosphatase antibody was used to detect the conjugation efficiency. To quantify goat anti-mouse-alkaline phosphatase antibody, 2 mg/mL of enzyme substrate para-nitrophenyl-phosphate (p-NPP, Ameresco, USA) in alkaline phosphatase buffer (100 mM Tris–HCl; 100 mM NaCl; 10 mM $MgCl_2$, pH 9.6) was added, and the bound proteins were quantified at 405 nm using a plate reader (Tecan, Sunrise, Australia). The content of cetuximab was calculated according to calibration curve.

### 2.3. Myelin preparation

Myelin preparation from adult rat spinal cord was produced according to previous study [17]. Briefly, the spinal cord of Sprague–Dawley (SD) rats was removed and homogenized in 0.3 M of sucrose. The suspension was layered over 0.85 M of sucrose and centrifuged at 27,000 g for 1 h. The sample was collected from the 0.32/0.85 M interface. The suspension and centrifugation procedures were repeated twice, and done in ice bath. After removal of excess sucrose, the resuspened myelin was filtered through a 0.22 μm filter (Corning, USA) to sterilize and remove any large aggregates.

### 2.4. NPC culture

NPCs were cultured as previously described with slight modification [18]. Briefly, the telencephalons were dissected from SD rats, cut into 1 $mm^3$ pieces, and digested in 0.25% trypsin at 37 °C for 40 min. Then trypsin inhibitor was added to stop the digestion, followed by centrifugation at 500 g for 5 min. The cell suspension was cultured in 25 $cm^2$ tissue culture flask (Corning, USA) in serum-free DMEM/F12 medium containing 20 ng/mL bFGF (Peprotech Asia, Rehovot, Israel), 20 ng/mL EGF (Peprotech Asia), 2% B27 (Invitrogen, GIBCO, NY, USA), 30% glucose (Sigma, USA), and 1.83 μg/mL heparin (Sigma, USA). After 7-day culture, neurospheres were enzymatically dissociated to single cells for the following experiments. The NPCs were resuspened in adhesion medium containing 10% FBS and $2 \times 10^6$ cells were seeded on collagen or col-cetuximab scaffolds. After 1-day culture, the adhesion medium was removed. After wash with PBS three times, differentiation medium containing 2% B27 and myelin proteins in DMEM/F12 medium was added. For NPC differentiation, collagen scaffolds functionalized with a series of dose of cetuximab were studied including col scaffold, col-cetuximab 0.5 μg scaffold (scaffold loaded with 0.5 μg of cetuximab initially), col-cetuximab 1 μg scaffold (scaffold loaded with 1 μg of cetuximab initially), col-cetuximab 2 μg scaffold (scaffold loaded with 2 μg of cetuximab initially).

### 2.5. Western blotting

After 7-day culture, the cells were collected and lysed by RIPA buffer (Sigma, USA) supplemented with proteinase inhibitor cocktail (04693116001, Roche Applied Science, Mannheim, Germany) for 30 min on ice after washed with PBS. The cell lysates were harvested from the supernatant from centrifugation at 12,000 g for 30 min. After quantification by BCA assay, 20 μg of protein was separated by sodium docecyl sulfate (SDS)-polyacrylamide gel, and transferred to a nitrocellulose membrane (GE, Amershame, Buckinghamshire, UK). The bolts were probed with indicated primary antibodies, followed by secondary antibodies conjugated with HRP. The primary antibodies used in this study included: anti-TUj1 (1:1000, 05-559, Millipore), anti-GFAP (1:1000, MAB360, Millipore), anti-S100 (1:500, Ab4066, Abcam), anti-β-actin (1:10,000, T5168, Sigma).

### 2.6. Immunocytochemistry

After 7-day culture in differentiation medium with/without myelin proteins, NPCs cultured on the scaffolds were fixed in 4% paraformaldehyde for 30 min, and permeabilized by 0.08% triton X-100 for 30 min. Then samples were blocked with 5% BSA in PBS for 1 h, and incubated with primary antibodies overnight at 4 °C. After wash with PBS three times, the samples were incubated with secondary FITC-conjugated antibodies and Hoechst 3342 (1 mg/mL) for 30 min at 37 °C. Primary antibodies were diluted as follow: anti-TUj1 at 1:400, and anti-GFAP at 1:500. After immunestaining, fluorescent images were taken with scanning laser confocal fluorescence microscope (A1RSi, Nikon).

### 2.7. Scanning electron microscopy (SEM) characterization

NPCs cultured scaffolds were fixed in 2% glutaraldehyde for 40 min at 4 °C. Subsequently, they were dehydrated in ethanol with a series of concentrations: 30%, 50%, 70%, 75%, 80%, 85%, 90%, and 95% for 10 min, and 100% for 20 min. The ethanol was extracted in 3:1, 1:1, and 1:3 mixtures of ethanol and amyl acetate for 20 min each followed by 100% amyl acetate storage for 20 min. Then the samples were dried by super critical $CO_2$ extraction, and coated with gold using a sputter. The images were captured by HITACHI S-3000N SEM (Hitachi, Tokyo, Japan).

### 2.8. Spinal cord hemisection

GFP–NPCs were obtained from GFP transgenic mouse for the following use in animal study. All animal procedures were performed in accordance with Chinese Ministry of Public Health (CMPH) Guide and US National Institute of Health (NIH) Guide for the care and use of laboratory animals. SD rats (200–220 g) were housed

in ventilated, humidity and temperature controlled (23–25 °C) rooms with a 12 h light/dark cycle. Standard food pellets and water were supplied. SCI was performed as described before with slight modification [12]. Briefly, following intraperitoneal anesthesia with sodium pentobarbital, a 2 cm midline incision was made along the vertebrae. After resecting the laminae, the spinal dura mater was incised to expose the spinal cord. A lateral hemisection at T13-L2 level was made by creating a 4-mm long longitudinal cut along the midline of the cord. Right after the SCI, the scaffolds (4-mm-long, 2-mm-diameter) were implanted into transected gap. All animals were divided into 4 groups accepting different treatments: col scaffolds, NPC-embedded col scaffold, NPC-embedded col-cetuximab 1 μg scaffold, NPC-embedded col-cetuximab 5 μg scaffold (scaffold loaded with 5 μg of cetuximab initially). Then, the surgery site was closed in layers.

### 2.9. Immunohistochemistry

After 4 weeks and 12 weeks, animals were perfused with 4% paraformaldehyde in PBS. Spinal cords were dissected, post-fixed overnight at 4 °C, and transferred to 20% sucrose (overnight at 4 °C) and then 30% sucrose (72 h at 4 °C). 1.5-cm-long horizontal sections of spinal cords containing the lesion/graft site were sectioned on a cryostat set at 20 μm thickness. The slides were fixed in acetone for 15 min at 4 °C, and then the samples were incubated in PBS containing 5% BSA with 0.1% Trition X-100 for 1 h at RT. The samples were incubated with primary antibodies: anti-GFP (1:200, ab290, Abcam), anti-GFAP (1:500, MAB360, Millipore), anti-MAP2 (1:200, M9942, Sigma), anti-neurofilament (NF, 1:100, ab3966, Abcam), and anti-synaptophysin (1:1000, MAB368, Millipore) overnight at 4 °C, and then incubated in Alexa 488 conjugated donkey anti-rabbit secondary antibody (1:500, A21206, Invitrogen) and Alexa 594 conjugated donkey anti-mouse secondary antibody (1:800, A21203, Invitrogen) for 1 h at RT. DAPI was used for nuclear staining.

### 2.10. Functional analysis

Locomotion recovery after SCI was scored in an open field according to Basso-Beattie-Bresnahan (BBB) locomotion rating scale of 0 (complete paralysis) to 21 (normal locomotion) [19]. Animals were allowed to move freely in an open area and the movements of hindlimb were examined and recorded for 5 min. The evaluation was performed by two observers blinded to the treatments weekly. For the inclined plane test, the highest degree of inclination was defined as being that at which the rats could maintain their position for 5 s on two separate trials [20].

### 2.11. Statistical analysis

The Data are presented as mean ± standard deviation. Multiple group comparisons were made using one-way analysis of variance (ANOVA). Two-group comparisons were tested by Student's test. * represented $p$ value $< 0.05$, **$p$ value $< 0.01$.

## 3. Results

### 3.1. Scaffold fabrication and characterization

The collagen scaffold showed a sponge-like structure, cylindrical shape and changeable size (Fig. 1A), suggesting that it could be an ideal candidate to bridge across the lesion site in SCI. The collagen scaffold was cut into disk-shaped pieces (4 mm in diameter, 1 mm in thickness) for *in vitro* study. Fig. 1B shows a representative SEM image of the collagen scaffold. The scaffold possessed lattice-like lamellae, high porosity of 98.6% and an interconnected porous structure with a pore size of 60–200 μm, which could provide sufficient space for cell adherence and growth. NPCs isolated from the telencephalons of neonatal rats proliferated and formed floating spheres in neurosphere medium containing growth factors (bFGF and EGF). A single-cell suspension digested by trypsin was seeded on the scaffolds. After NPC attachment, the adhering medium with FBS was replaced. After 7 days of culture, cell growth on the collagen scaffold was examined via fluorescein diacetate (FDA) staining and SEM analysis. The FDA fluorescence staining (Fig. 1C) showed that the cells adhered and grew well on the scaffold with a high population and good distribution. The SEM analysis (Fig. 1D) showed that the cells grew inside the pore, and spread well on the wall. These findings indicated that the collagen scaffold was well-suited as scaffold for NPC delivery in SCI repair.

### 3.2. EGFR antagonist functionalization

Hetero-bi-functional corss-linker Sulfo-SMCC and Traut's Reagent were used to conjugate cetuximab on the collagen scaffolds to create a functional scaffold which could specifically block EGFR. Fig. 2A schematically illustrates the facile conjugation of EGFR

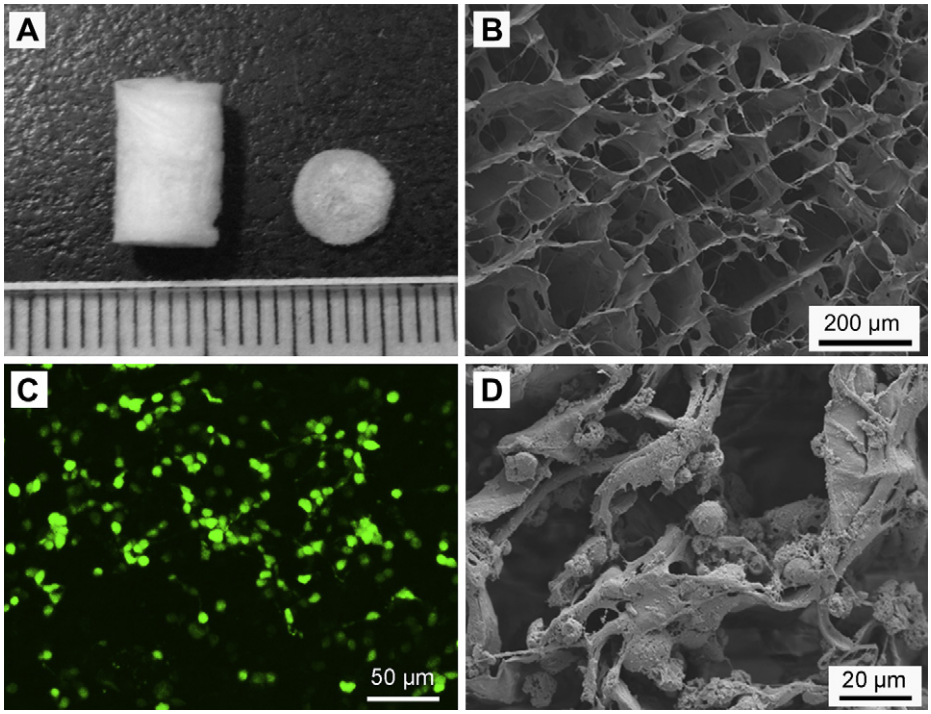


**Fig. 1.** (A) Picture displayed the structure of the collagen scaffold with a diameter of 4 mm. (B) SEM image showing the morphology of porous collagen scaffold. (C) Confocal image of FDA staining and (D) SEM image of NPCs cultured on collagen scaffold for 7 days.

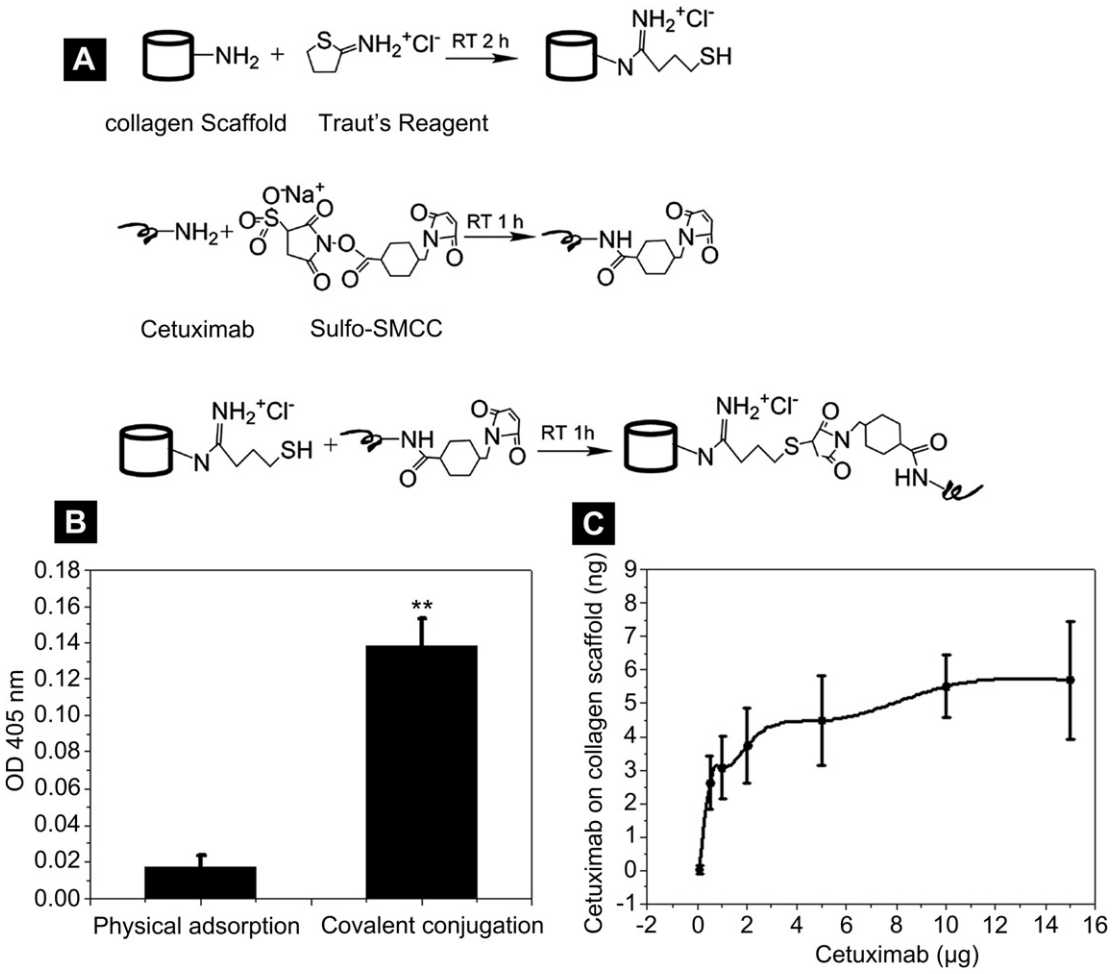


**Fig. 2.** (A) Schematic illustration of cetuximab conjugation on colllagen scaffold by using Traut's Reagent and Sulfo-SMCC. (B) Cetuximab binding ability via physical and chemical conjugation measured by ELISA assay. (C) Cetuximab binding curve on collagen scaffold with varied loading content. The data are expressed as mean ± standard deviation for $n = 3$. $^{**}P < 0.01$.

antibody with collagen scaffold, both of which are rich in amino groups. The cetuximab immobilized on the scaffold was detected by enzyme-linked immunosorbent assay. As shown in Fig. 2B, more cetuximab was retained on the scaffolds by using covalent conjugation compared with that of physical adsorption, suggesting that chemical covalent bond between collagen and antibody is substantial for antibody immobilization. Fig. 2C shows the cetuximab binding curve on collagen scaffolds with varied loading content. It can be seen that the amount of bound antibodies on scaffolds increased in a dose dependent manner. The cetuximab on the scaffold increased significantly at the first stage, and reached a plateau when the input loading content exceeded 5 μg.

### 3.3. Prepared myelin proteins inhibited neuronal differentiation of NPCs in vitro

Although transplantation of NPCs holds the promise, the regeneration ability was limited in adult SCI largely due to the inhibitory milieu. To mimic growth-inhibitory environment in SCI, SCI myelin proteins were added in the culture medium for NPC culture. Fig. 3A shows the MTT assay of NPCs with different concentration of myelin proteins. It was found that myelin proteins markedly promoted the cell proliferation and the cell number was highest at concentration of 5 μg/mL. We further assessed the effect of myelin on NPC differentiation. Fig. 3B shows representative images of TUj-1 and GFAP immunostaining of NPCs exposed to 1, 2, and 5 μg/mL of myelin after differentiating for 7 days. The expression of neuron marker TUj-1 was much lower in the myelin groups, and whereas, the expression of glia marker GFAP was higher. Quantitative results, as shown in Fig. 3C, showed that percentages of TUj-1 positive cells decreased from around 37% (without myelin) to 31% (1 μg/mL of myelin), 23% (2 μg/mL of myelin), and 20% (5 μg/mL of myelin). Meanwhile, percentages of GFAP positive cells increased from around 50% (without myelin) to 53% (1 μg/mL of myelin), 54% (2 μg/mL of myelin), and 57% (5 μg/mL of myelin) (Fig. 3D). Based on the MTT and differentiation results, myelin concentration of 5 μg/mL has been demonstrated to be favorable for cell growth and efficient for suppressing neuronal differentiation. Therefore, 5 μg/mL of myelin was used in the following *in vitro* experiments.

### 3.4. Col-cetuximab scaffolds promoted neuronal differentiation and inhibited astrocytic differentiation of NPCs in vitro

Differentiation of NPCs cultured on collagen scaffolds with a series of dose of cetuximab was studied in the presence of 5 μg/mL of myelin in the culture medium. Immunostaining results showed that the expression of TUj-1, the marker of neurons, was increased on col-cetuximab 0.5 μg scaffold and col-cetuximab 1 μg scaffold, and decreased on the col-cetuximab 2 μg scaffold, meanwhile, the

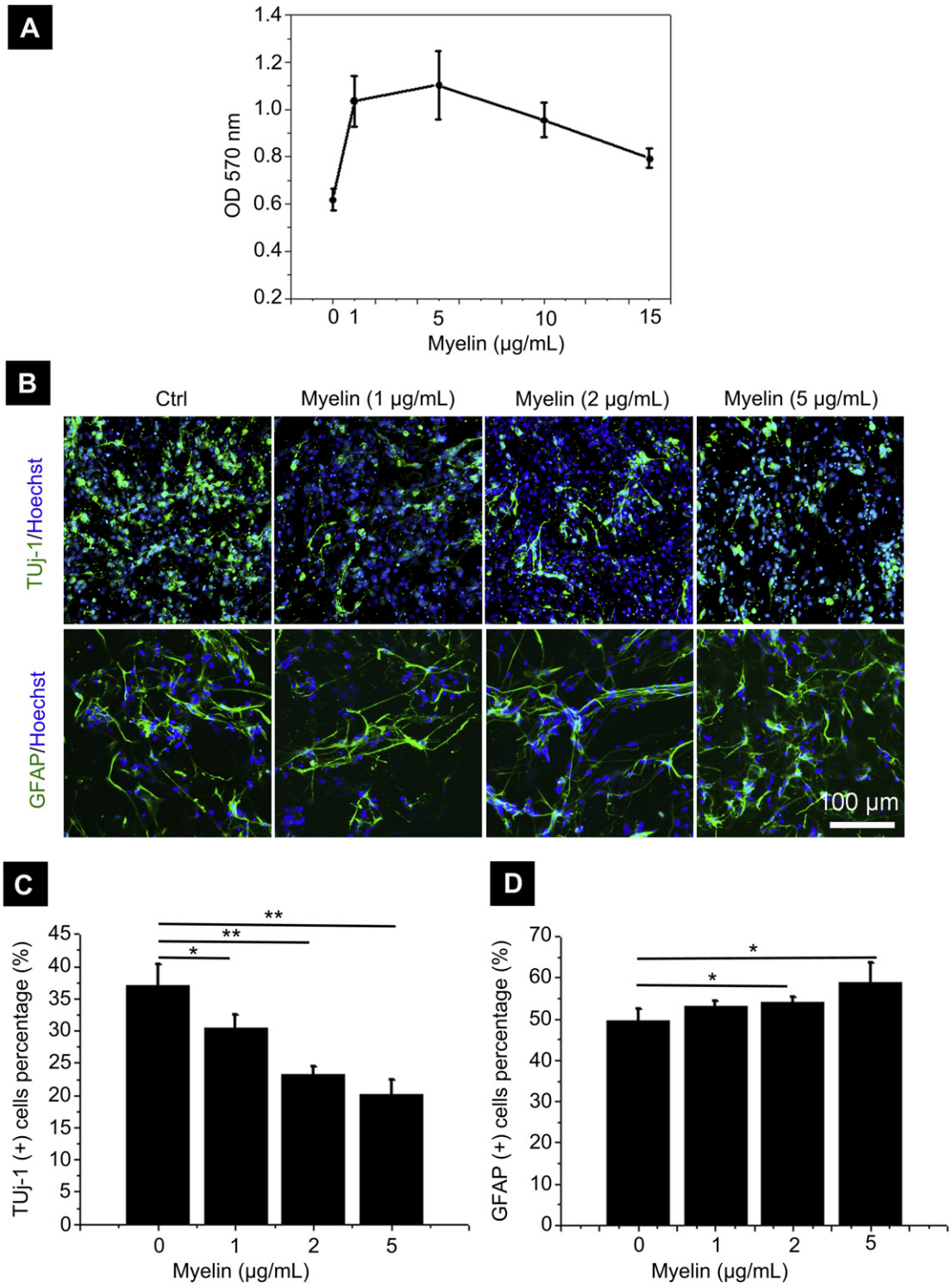


**Fig. 3.** The effect of myelin on cell number and differentiation of NPCs. (A) MTT measurement showed that myelin markedly promoted the cell proliferation. (B) Representative images of TUj-1$^+$ (for neurons) and GFAP$^+$ (for astrocytes) immunostaining of NPCs treated by varied concentration of myelin for 7 days. (C) TUj-1$^+$ and (D) GFAP$^+$ quantification. Scale bar, 100 μm. $^*P < 0.05$, $^{**}P < 0.01$.

expression of GFAP, the marker of astrocytes, was decreased on all col-cetuximab scaffolds (Fig. 4A). Percentages of TUj-1 positive cells increased from around 21% (collagen scaffold alone) to 28% (col-cetuximab 0.5 μg scaffold), and 34% (col-cetuximab 1 μg scaffold), and decreased to 18% (col-cetuximab 2 μg scaffold), indicating that functionalization with appropriate amount of cetuximab resulted in a more neuronal population (Fig. 4B). Percentages of GFAP positive cells decreased from around 55% (collagen scaffold alone) to 53% (col-cetuximab 0.5 μg scaffold), 48% (col-cetuximab 1 μg scaffold) and 40% (col-cetuximab 2 μg scaffold), indicating that the col-cetuximab scaffolds inhibited the astrocytic differentiation of NPCs (Fig. 4C). The staining results were further confirmed by

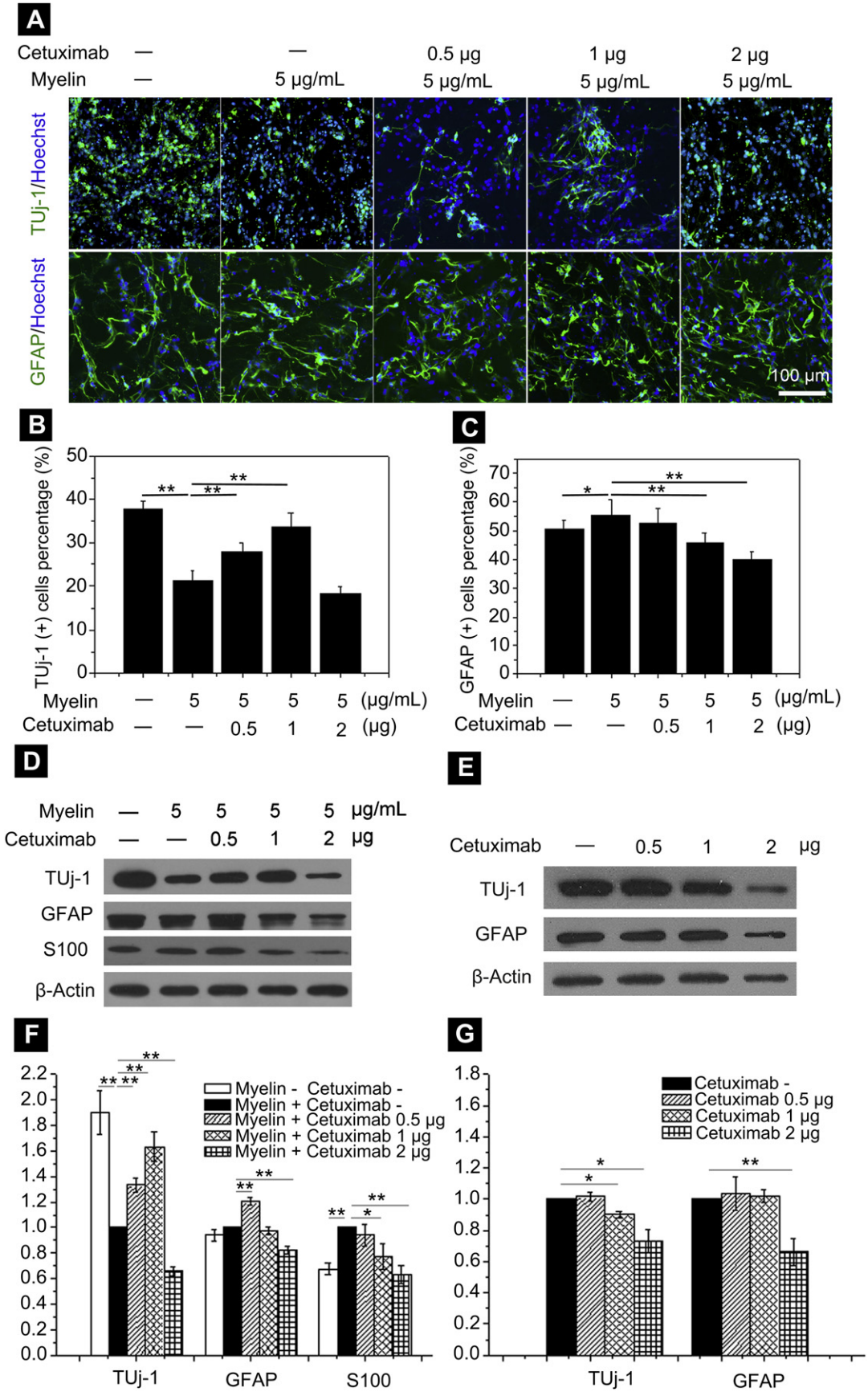


**Fig. 4.** Cetuximab-cunjugated collagen scaffold promoted neuronal differentiation and inhibited astrocytic differentiation of NPCs exposed to 5 μg/mL of myelin. (A) Representative images of TUj-1$^+$ and GFAP$^+$ immunostaining of NPCs cultured on scaffolds exposed to myelin for 7 days. (B) TUj-1$^+$ and (C) GFAP$^+$ quantification. (D, E) Western blot analysis of TUj-1$^+$, GFAP$^+$ and S100$^+$ of NPCs cultured on scaffolds with (D) and without (E) myelin in the culture medium. (F) and (G) quantitation of protein bands in (D) and (E) respectively. Scale bar, 100 μm. $^*P < 0.05$, $^{**}P < 0.01$.

western blot analysis (Fig. 4D,F). In col-cetuximab scaffold groups, GFAP expression was down-regulated gradually, with 8% and 18% decrease in col-cetuximab 1 μg scaffold group and col-cetuximab 2 μg scaffold group respectively. Similarly, S100, another marker of astrocytes, showed significant down-regulation, with 23% and 37% decrease in col-cetuximab 1 μg scaffold group and col-cetuximab 2 μg scaffold group respectively. The consistent results revealed a decreased astrocytic differentiation on col-cetuximab scaffolds. Whereas, TUj-1 expression was up-regulated by 33% and 63% for col-cetuximab 0.5 μg scaffold group and col-cetuximab 1 μg scaffold group respectively, and down-regulated by 34% for col-cetuximab 2 μg scaffold group. It can be concluded that functionalization with appropriate amount of cetuximab was helpful for neuronal differentiation. Therefore, to deeper understand the effect of EGFR antibody on neuronal differentiation of NPCs, we examined NPC differentiation on col-cetuximab scaffolds without the intervention of myelin (Fig. 4E,G). The decreased neuronal differentiation suggested that overdose of cetuximab which is above the amount that overcomes the effect of myelin proteins would reduce the neuronal differentiation. Taken together, collagen scaffolds functionalized with a defined amount of cetuximab (col-cetuximab 1 μg scaffold in this work) was capable of enhancing neuronal differentiation as well as inhibiting astrocytic differentiation of NPCs exposed to myelin proteins.

### 3.5. Col-cetuximab scaffolds increased neuronal differentiation, decreased astrocytic differentiation of implanted NPCs, and promoted functional recovery post-SCI

Surgical procedures of SCI are shown in Fig. 5A–D. Rats were subjected to T13-L2 spinal cord hemisection in which 4 mm of tissue was removed (Fig. 5A,B). Right after the injury, the lesions were bridged with col scaffold, GFP-NPC embedded col scaffold, GFP-NPC embedded col-cetuximab 1 μg scaffold or GFP-NPC embedded col-cetuximab 5 μg scaffold (Fig. 5C,D). Behavioral analysis was performed to rate open-field locomotion by BBB scale. Immediately

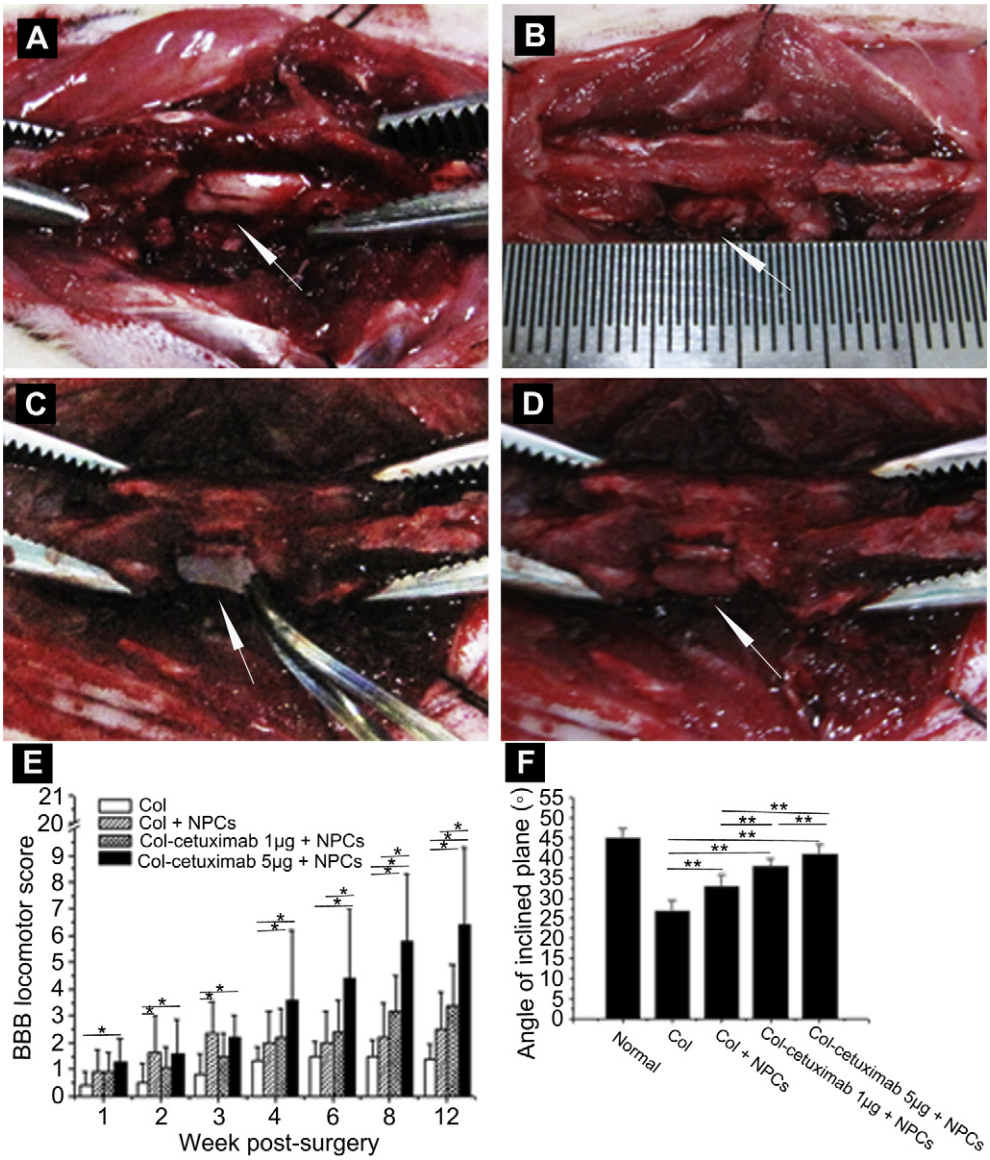


**Fig. 5.** Surgical procedures of hemisection SCI model and behavioral outcome post-SCI. (A) The exposed hemi-spinal cord of rats. (B) The hemi-transection site. (C) The implantation of scaffolds with or without NPCs. (D) The transection site filled with scaffolds. (E) Hindlimb locomotion: BBB scores. (F) Inclined plane results at 12 weeks post-SCI. $^{*}P < 0.05$, $^{**}P < 0.01$.

after surgery, BBB score of every rat was approximately 0, suggesting that the SCI model was successful. As shown in Fig. 5E, the recovery was improved by the intervention of scaffold plus NPCs, while the scaffold alone group only had modest effect. At 12 weeks post-implantation, the BBB score of NPC-embedded col-cetuximab 5 μg scaffold group reached a level of 6.4, indicating movement about each point of the hindlimb. Inclined plane performance was tested for their ability to maintain body position on an inclined plane (Fig. 5F). Consistently, the NPC-embedded col-cetuximab 5 μg scaffold group showed statistically significant improvement.

Next, we performed immunostaining through the spinal cord lesion to assess the NPC fate *in vivo*. Fig. 6A shows the overview of transected region in NPC-embedded col-cetuximab 5 μg scaffold group at 12 weeks post-implantation. It can be seen that the implant almost filled the lesion cavity and integrated with host tissue. An enlarged image, shown in Fig. 6B, confirmed the great host tissue-implant integration. Fig. 6C and D show the double immunostaining of MAP2/GFP, and GFAP/GFP respectively. We found that GFP-labeled cells co-localized with the mature neuronal marker MAP2 (microtubule associated protein 2), and astrocyte marker GFAP, indicating that implanted NPCs could differentiate into neurons and astrocytes in the surroundings of lesion site. Notably, NPCs on col-cetuximab 5 μg scaffolds expressed distinct level of MAP2, but lower level of GFAP compared with those on collagen scaffolds. Quantitative analysis showed that percentages of MAP2 positive cells were 13%, 14% and 25% in GFP positive NPCs for col, col-cetuximab 1 μg, and col-cetuximab 5 μg scaffolds treated groups respectively at 4 weeks post-SCI. The percentages of MAP2 positive cells increased at 12 weeks post-SCI, accounting for 14%, 15% and 27% respectively. Whereas, percentages of GFAP positive cells were 34%, 28% and 21% respectively at 4 weeks post-SCI, and 30%, 27% and 16% respectively at 12 weeks post-SCI (Fig. 6E). The quantitative results revealed a significant increase in MAP2 positive mature neurons and dramatic decrease in GFAP positive astrocytes for NPCs on the col-cetuximab 5 μg scaffold group, indicating that col-cetuximab 5 μg scaffold favored neuronal differentiation, and suppressed astrocytic differentiation. In addition to expressing mature neuronal markers, GFP-NPCs extended axons, as demonstrated by co-labeling for the axonal marker neurofilament (Fig. 7A). There was much more NF positive axons on the col-cetuximab 5 μg scaffold group than the collagen scaffold group. Additionally, double immunofluorescent labeling for GFP and synaptophysin suggested synapse formation between neurons (Fig. 7B). It can be seen that col-cetuximab 5 μg scaffold group possessed more pronounced enhancement in synapse formation.

## 4. Discussion

Although NPCs have the potential for neuronal differentiation *in vitro*, the majority of implanted NPCs differentiate into astrocytic phenotype in the lesion site. Recently, myelin-associated proteins, which involved in the niche for NPCs after SCI, have been demonstrated to induce astrocytic differentiation of grafted NPCs rather than neuronal differentiation [8]. Evidences showed that inhibition of EGFR, downstream signaling activated by myelin associated inhibitors, could benefit SCI regeneration, however, little is known about the influence of EGFR inhibition on fate decision of NPCs. Inhibition of EGFR was recently found to induce neuronal differentiation from NG2+ glial progenitors, and promote functional recovery in mouse contusive SCI [21]. It could be of great significance to determine whether inhibition of EGFR signaling would benefit neuronal differentiation from NPCs after SCI. In this study, we aimed to fabricate a functionalized scaffold suitable for NPC transplantation in SCI repair. Herein, cetuximab, an EGFR antibody, immobilized collagen scaffold was developed for NPC implantation in SCI repair.

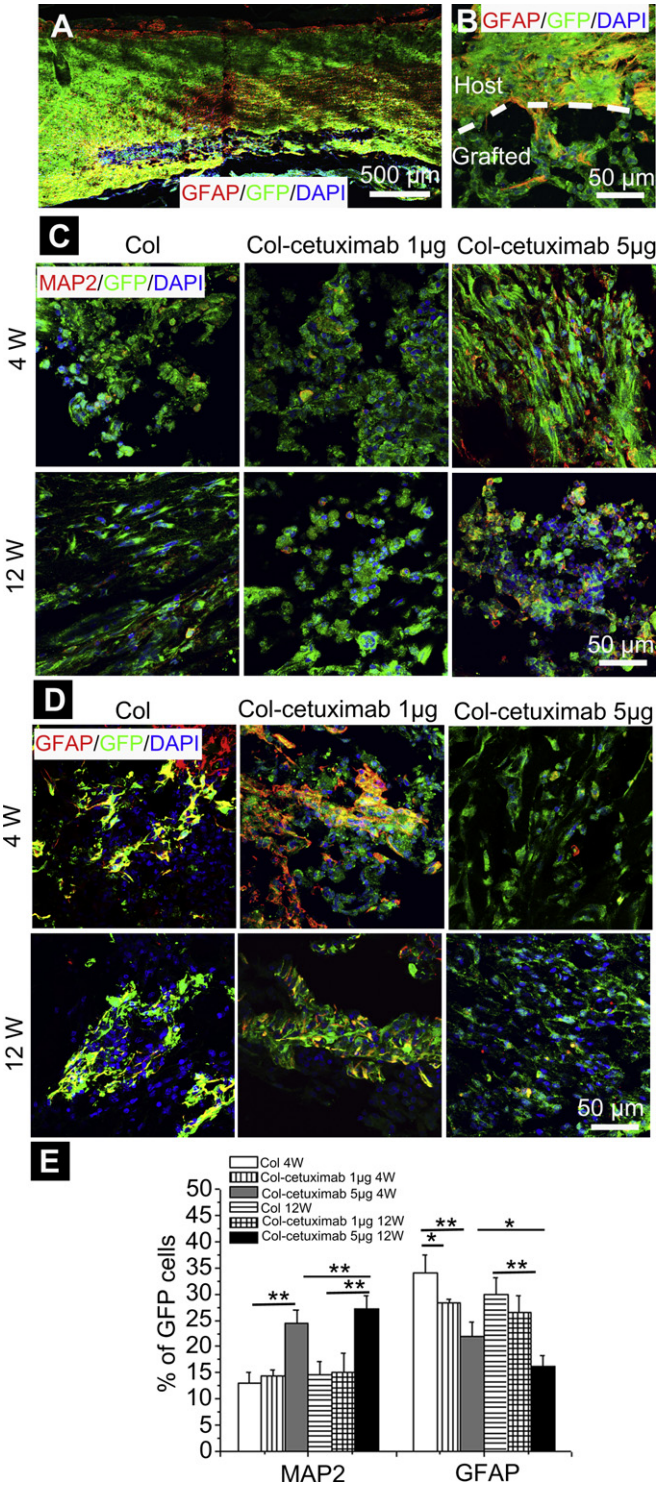


**Fig. 6.** Differentiation of NPCs in hemi-transection site. (A) Overview and (B) an enlarged image of NPC-embedded col-cetuximab 5 μg scaffold group at 12 weeks post-SCI, showing great integration and filling of the lesion site. (C) Immunostaining ($MAP2^+/GFP^+$) images showing neuronal differentiation of the grafted cells. (D) Immunostaining ($GFAP^+/GFP^+$) images showing astrocytic differentiation of the grafted cells. (E) Neuronal and astrocytic phenotype quantification. Scale bars, (A) 500 μm, (B–D) 50 μm. $^*P < 0.05$, $^{**}P < 0.01$.

Porous collagen scaffold was used as vehicle for NPC and EGFR antagonist delivery owing to its good biocompatibility, large space for cell accommodation and well-demonstrated use in neural tissue engineering [22–24] (Fig. 1). Cetuximab, the EGFR antagonist, which is

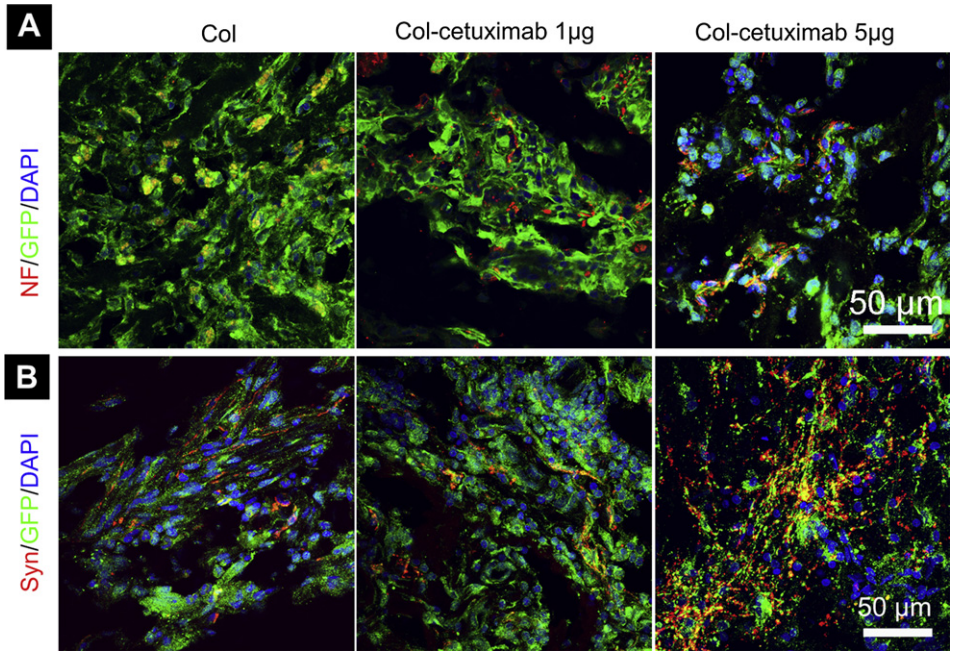


**Fig. 7.** Representative images of GFP$^+$-grafted cells labeled with the (A) neurofilament (NF$^+$) and (B) synaptophysin (Syn$^+$) at 12 weeks post-SCI. Scale bars, 50 μm.

widespreadly used in clinical practice [25] was covalently crosslinked onto the scaffolds (Fig. 2). Covalent modification of biochemical molecules to the scaffolds has been demonstrated to improve its clinical therapy effectiveness due to the effective local concentration, prolonged availability and decreased risk of high dose as compared with the injection or mini-pump administration at the lesion [26].

SCI myelin proteins were prepared to mimic the growth-inhibitory environment after SCI. The outcome of inhibited neuronal differentiation and enhanced astrocytic differentiation of NPCs (Fig. 3) was consistent with the finding *in vivo* that adult spinal cord provides molecular cues for gial, but for neuronal differentiation for NPC transplantation [27]. We then examined the NPC differentiation on col-cetuximab scaffolds in presence and absence of myelin proteins *in vitro* (Fig. 4). It was found that col-cetuximab scaffolds decreased the astrocytic differentiation of NPCs. Meanwhile, TUj-1 antibody was used to identify the differentiated neurons in immunostaining and western blotting analysis. Encouragingly, the inhibited neuronal differentiation induced by myelin proteins was recovered partially on the scaffolds functionalized with appropriate amount of cetuximab (col-cetuximab 1 μg scaffold in this work). It was found that on col-cetuximab 2 μg scaffolds in presence of myelin proteins, and all col-cetuximab scaffolds in absence of myelin, a decrease in neuronal differentiation of NPCs was observed, indicating that overdose of cetuximab that exceeded the amount required for overcoming the effect of myelin proteins would decrease the neuronal differentiation. EGFR signaling has been demonstrated to play an important role in neuronal survival [28]. Therefore, impaired EGFR signaling which might cause neuron death could be a possible reason for the reduced neuronal differentiation on col-cetuximab 2 μg scaffold in presence of myelin proteins. From these results, we concluded that collagen scaffold immobilized with defined amount of cetuximab could neutralize the inhibitory activity of myelin proteins, resulting in an enhanced neuronal differentiation and decreased astrocytic differentiation *in vitro*.

We subsequently evaluated whether NPCs embedded on col-cetuximab scaffolds may acquire more neuronal phenotypes *in situ*, and subsequently promote functional recovery post-SCI. It was found that the construct comprised of porous collagen scaffold, cetuximab functionalization and NPCs was effective in promoting neural regeneration following hemisection of the rat spinal cord. The locomotion recovery was assessed by the BBB score (Fig. 5E). It was found that the intervention of scaffold plus NPCs could help improve the functional outcome, but appeared not sufficient. When combined with cetuximab functionalization on the scaffold, significant recovery was achieved. Inclined plane results (Fig. 5F) mirrored the BBB scoring, indicating that implantation of NPC-embedded col-cetuximab 5 μg scaffold could lead to the long-term improvement of motor function significantly.

We further sought to determine the basis for this improvement in locomotor function. The immunostaining results showed that NPCs on col-cetuximab 5 μg scaffolds differentiated into more neurons and fewer astrocytes compared with that on collagen scaffolds at 4 weeks and 12 weeks post-SCI (Fig. 6). It can be seen that the neuronal differentiation was enhanced and astrocytic differentiation was reduced further with longer observation. This finding was consistent with the previous study that suppression of the gliogenic determinants allowed the differentiation of NPCs toward a neurogenic fate post CNS injury [29]. The neurons derived from transplanted neural stem cells have been demonstrated to restore disrupted neuronal circuitry, and contribute to functional improvements post-SCI [30]. On the other hand, it has been demonstrated that the reactive astrocytes could migrate towards the injured area to constitute the glial scar after SCI and hinder functional recovery [31]. Therefore, we can conclude that the col-cetuximab scaffold could stimulate implanted NPC into neuronal phenotypes rather than astrocytic phenotypes, and subsequently, the accumulation of newly generated neurons, and attenuation of astrocytes contributed to a better functional recovery.

Additionally, the lesion site was also stained with other neuronal markers i.e. NF and synaptophysin (Fig. 7). Enhanced axon generation and synapse formation were observed on the col-cetuximab 5 μg scaffolds. The projection of NPC-derived axons from the lesion site together with synapse formation also contributed to the enhanced functional recovery.

Here, we demonstrated that col-cetuximab scaffolds could promote neuronal differentiation and inhibit astrocytic differentiation

of NPCs exposed to myelin proteins *in vitro* and *in vivo* post-SCI. The highly activated EGFR signaling post-SCI, which is considered as one of gliogenic signaling for NPCs, could be significantly suppressed by cetuximab, which released from the col-cetuximab scaffolds. Under this circumstance, more implanted NPCs could acquire neuronal phenotypes with the inhibition of EGFR activity.

## 5. Conclusions

In summary, we have demonstrated that cetuximab, an EGFR antibody, functionalized collagen scaffold could rescue NPCs from adverse effect induced by myelin proteins, direct neuronal differentiation of NPCs, and eventually promote functional recovery after SCI. When in presence of 5 μg/mL of myelin in the culture medium, the TUj-1 expression of NPCs on the col-cetuximab 1 μg scaffold was up-regulated by 63%, and GFAP and S100 expression were down-regulated by 8% and 23% respectively as compared with that on collagen scaffold. Furthermore, the therapeutic test in rat hemisection SCI model showed that the NPC-embedded col-cetuximab 5 μg scaffold caused a wide range of positive effects, including enhanced neuronal differentiation and decreased astrocytic differentiation of NPCs, promoted axonal regeneration and synapse formation, and improved functional recovery. Thus, functionalization of collagen scaffold with well-defined amount of EGFR antibody appears a suitable scaffold to positively mediate NPC differentiation in SCI repair. This engineered collagen scaffold provides a platform in which additional stimuli can be introduced to improve the recovery after SCI.

## Acknowledgments

This work was supported by grants from the Ministry of Science and Technology of China (2011CB965001), National Science Foundation of China (81200963, 30930032) and Chinese Academy of Sciences (KSCX2- EW-Q-24).

## Abbreviations

| | |
|---|---|
| NPC | neural progenitor cell |
| SCI | spinal cord injury |
| EGFR | epidermal growth factor receptor |
| MAG | myelin associated glycoprotein |
| OMgp | oligodendrocyte-myelin glycoprotein |
| NgR | Nogo recptor |
| CNS | central nervous system |
| p-NPP | para-nitrophenyl-phosphate |
| SEM | Scanning electron microscopy |
| BBB | Basso-Beattie-Bresnahan |
| FDA | fluorescein diacetate |
| MTT | 3-(4,5-Dimethyl-2-thiazolyl)-2,5-diphenyl-2H-tetrazolium bromide |
| NF | neurofilament |

## References

[1] Cusimano M, Biziato D, Brambilla E, Donega M, Alfaro-Cervello C, Snider S, et al. Transplanted neural stem/precursor cells instruct phagocytes and reduce secondary tissue damage in the injured spinal cord. Brain 2012;135:447–60.
[2] Ronaghi M, Erceg S, Moreno-Manzano V, Stojkovic M. Challenges of stem cell therapy for spinal cord injury: human embryonic stem cells, endogenous neural stem cells, or induced pluripotent stem cells? Stem Cells 2010;28:93–9.
[3] Aboody K, Capela A, Niazi N, Stern JH, Temple S. Translating stem cell studies to the clinic for CNS repair: current state of the art and the need for a rosetta stone. Neuron 2011;70:597–613.
[4] Kim H, Cooke MJ, Shoichet MS. Creating permissive microenvironments for stem cell transplantation into the central nervous system. Trends Biotechnol 2012;30:55–63.
[5] Stabenfeldt SE, Munglani G, García AJ, LaPlaca MC. Biomimetic microenvironment modulates neural stem cell survival, migration, and differentiation. Tissue Eng Part A 2010;16:3747–58.
[6] Lu P, Wang Y, Graham L, McHale K, Gao M, Wu D, et al. Long-distance growth and connectivity of neural stem cells after severe spinal cord injury. Cell 2012;150:1264–73.
[7] Akbik F, Cafferty WBJ, Strittmatter SM. Myelin associated inhibitors: a link between injury-induced and experience-dependent plasticity. Exp Neurol 2012;235:43–52.
[8] Wang B, Xiao Z, Chen B, Han J, Gao Y, Zhang J, et al. Nogo-66 promotes the differentiation of neural progenitors into astroglial lineage cells through mTOR-STAT3 pathway. PLoS One 2008;3:e1856.
[9] Wang T, Wang J, Yin C, Liu R, Zhang JH, Qin X. Down-regulation of Nogo receptor promotes functional recovery by enhancing axonal connectivity after experimental stroke in rats. Brain Res 2010;1360:147–58.
[10] Xu CJ, Xu L, Huang LD, Li Y, Yu PP, Hang Q, et al. Combined NgR vaccination and neural stem cell transplantation promote functional recovery after spinal cord injury in adult rats. Neuropathol Appl Neurobiol 2011;37:135–55.
[11] Koprivica V, Cho KS, Park JB, Yiu G, Atwal J, Gore B, et al. EGFR activation mediates inhibition of axon regeneration by myelin and chondroitin sulfate proteoglycans. Science 2005;310:106–10.
[12] Han Q, Jin W, Xiao Z, Ni H, Wang J, Kong J, et al. The promotion of neural regeneration in an extreme rat spinal cord injury model using a collagen scaffold containing a collagen binding neuroprotective protein and an EGFR neutralizing antibody. Biomaterials 2010;31:9212–20.
[13] Qu W, Tian D, Guo Z, Fang J, Zhang Q, Yu Z, et al. Inhibition of EGFR/MAPK signaling reduces microglial inflammatory response and the associated secondary damage in rats after spinal cord injury. J Neuroinflamm 2012;9:178.
[14] Li ZW, Tang RH, Zhang JP, Tang ZP, Qu WS, Zhu WH, et al. Inhibiting epidermal growth factor receptor attenuates reactive astrogliosis and improves functional outcome after spinal cord injury in rats. Neurochem Int 2011;58:812–9.
[15] Ayuso-Sacido A, Moliterno JA, Kratovac S, Kapoor GS, O'Rourke DM, Holland EC, et al. Activated EGFR signaling increases proliferation, survival, and migration and blocks neuronal differentiation in post-natal neural stem cells. J Neuro-Oncol 2010;97:323–37.
[16] Berry M, Ahmed Z, Douglas MR, Logan A. Epidermal growth factor receptor antagonists and CNS axon regeneration: mechanisms and controversies. Brain Res Bull 2011;84:289–99.
[17] Norton WT, Poduslo SE. Myelination in rat brain: method of myelin isolation. J Neurochem 1973;21:749–57.
[18] Han J, Xiao Z, Chen L, Chen B, Li X, Han S, et al. Maintenance of the self-renewal properties of neural progenitor cells cultured in three-dimensional collagen scaffolds by the REDD1-mTOR signal pathway. Biomaterials 2013;34:1921–8.
[19] Basso DM, Beattie MS, Bresnahan JC. A sensitive and reliable locomotor rating scale for open field testing in rats. J Neurotrauma 1995;12:1–21.
[20] Rivlin AS, Tator CH. Objective clinical assessment of motor function after experimental spinal cord injury in the rat. J Neurosurg 1977;47:577–81.
[21] Ju P, Zhang S, Yeap Y, Feng Z. Induction of neuronal phenotypes from NG2+ glial progenitors by inhibiting epidermal growth factor receptor in mouse spinal cord injury. Glia 2012;60:1801–14.
[22] Davidenko N, Gibb T, Schuster C, Best SM, Campbell JJ, Watson CJ, et al. Biomimetic collagen scaffolds with anisotropic pore architecture. Acta Biomater 2012;8:667–76.
[23] Yu H, Cao B, Feng M, Zhou Q, Sun X, Wu S, et al. Combinated transplantation of neural stem cells and collagen type I promote functional recovery after cerebral ischemia in rats. Anat Rec 2010;293:911–7.
[24] Cholas RH, Hsu HP, Spector M. The reparative response to cross-linked collagen-based scaffolds in a rat spinal cord gap model. Biomaterials 2012;33:2050–9.
[25] Vale CL, Tierney JF, Fisher D, Adams RA, Kaplan R, Maughan TS, et al. Does anti-EGFR therapy improve outcome in advanced colorectal cancer? A systematic review and meta-analysis. Cancer Treat Rev 2012;38:618–25.
[26] Wolinsky JB, Colson YL, Grinstaff MW. Local drug delivery strategies for cancer treatment: gels, nanoparticles, polymeric films, rods, and wafers. J Control Release 2012;159:14–26.
[27] Vroemen M, Aigner L, Winkler J, Weidner N. Adult neural progenitor cell grafts survive after acute spinal cord injury and integrate along axonal pathways. Eur J Neurosci 2003;18:743–51.
[28] Wagner B, Natarajan A, Grunaug S, Kroismayr R, Wagner EF, Sibilia M. Neuronal survival depends on EGFR signaling in cortical but not midbrain astrocytes. EMBO J 2006;25:752–62.
[29] Geoffroy CG, Critchley JA, Castro DS, Ramelli S, Barraclough C, Descombes P, et al. Engineering of dominant active basic Helix-Loop-Helix proteins that are resistant to negative regulation by postnatal central nervous system anti-neurogenic cues. Stem Cells 2009;27:847–56.
[30] Abematsu M, Tsujimura K, Yamano M, Saito M, Kohno K, Kohyama J, et al. Neurons derived from transplanted neural stem cells restore disrupted neuronal circuitry in a mouse model of spinal cord injury. J Clin Invest 2010;120:3255–66.
[31] Buffo A, Rolando C, Ceruti S. Astrocytes in the damaged brain: molecular and cellular insights into their reactive response and healing potential. Biochem Pharmacol 2010;79:77–89.